



# **Final Report**

Project title: Energy band gap engineering of perovskite oxides for photocatalytic hydrogen production from visible light: Theory and computations

By Asst. Prof. Pakpoom Reunchan

## **Final Report**

Project title: Energy band gap engineering of perovskite oxides for photocatalytic hydrogen production from visible light: Theory and computations

## Researcher Institute

1. Asst. Prof. Pakpoom Reunchan Kasetsart University

2. Prof. Sukit Limpijumnong Suranaree University of Technology

This project granted by the Thailand Research Fund

Abstract

Project Code: TRG5780260

Project Title: Energy band gap engineering of perovskite oxides for photocatalytic hydrogen production from

visible light: Theory and computations

Investigator: Pakpoom Reunchan

E-mail Address : pakpoom.r@ku.ac.th

Project Period: 15 July 2014 to 14 July 2016

Abstract:

Density functional calculations are performed to investigate the effect of nitrogen (N) impurities on the optical properties of N-doped CaTiO<sub>3</sub>, SrTiO<sub>3</sub> and BaTiO<sub>3</sub>. The screened hybridfunctional proposed by Heyd, Scuseria, and Ernzherhof (HSE) is used to obtain the accurate band gaps, electronic structure and formation energies of the N impurities. In this project, we pay special attention to the energetics and optical properties of N impurities in SrTiO3, which is a promising candidate for hydrogen evolution under visible-light irradiation. Here, hybrid density-functional calculations are employed to investigate the stability and impact of nitrogen impurities on the electronic and optical properties in SrTiO<sub>3</sub>. We find that the substitutional N on O site (N<sub>O</sub>) is a deep acceptor in  $SrTiO_3$ .  $N_O$  predominates over other N-related defects under any equilibrium growth conditions in n-type  $SrTiO_3$ . Our results reveal that  $N_O$  gives rise to visible-light absorption, in agreement with experimental observations. In addition, we find that hydrogen can bind to No, and that N<sub>O</sub>-H<sub>i</sub> leads to a blueshift in the optical absorption. Other N configurations can also contribute to optical absorption in the visible range. The vibration frequencies of the different N configurations are provided to support identification by vibrational spectroscopy techniques.

Keywords: density-functional calculations, strontium titanate, doping, nitrogen

รหัสโครงการ: TRG5780260

ชื่อโครงการ: การออกแบบและปรับปรุงแถบช่องว่างพลังงานของเพอรอฟสไกต์ออกไซด์เพื่อการผลิต ไฮโดรเจนจากกระบวนการเร่งปฏิกิริยาด้วยแสงในย่านที่ตามองเห็น: ทฤษฎีและการคำนวณ

ผู้วิจัยหลัก: ผศ.ดร. ภาคภูมิ เรือนจันทร์

อีเมล์ : pakpoom.r@ku.ac.th

ระยะเวลาโครงการ : เริ่มตั้งแต่ 15 กรกฎาคม 2014 ถึง 14 กรกฎาคม 2016

บทคัดย่อ:

ในโครงการวิจัยนี้การคำนวณโดยใช้ฟังก์ชันนัลของความหนาแน่นถูกนำมาใช้ในการตรวจสอบคุณ สมบัติเชิงแสงของรูปแบบของสิ่งเจือปนในโตรเจนในแคลเซียมไททาเนต (CaTiO<sub>3</sub>) สตรอนเทียมไททาเนต (SrTiO<sub>3</sub>) และ แบเรียมไททาเนต (BaTiO<sub>3</sub>) ฟังก์ชันนัลแบบผสมที่ถูกกำบังเสนอโดย Heyd, Scusecria และ Ernzerhof (HSE)

ถูกน้ำมาใช้ในการคำนวณเพื่อให้ได้มาซึ่งแถบช่องว่างพลังงานของสารประกอบเพอรอฟไกส์ที่แม่นยำขึ้น รวมถึงโครงสร้างทางอิเล็กทรอนิกส์ และพลังงานการก่อตัวของความบกพร่องที่เกี่ยวข้องกับในโตรเจน ในโครงการวิจัยนี้ผู้วิจัยมุ่งเน้นไปที่การพลังงานของการก่อตัวและคุณสมบัติเชิงแสงของความบกพร่องและ ในโตรเจนที่เจือปนเข้าไปในผลึก SrTiO

ซึ่งเป็นวัสดุที่มีศักยภาพสำหรับการผลิตไฮโดรเจนภายใต้การแผ่ของแสงในย่านที่ตามองเห็น ในงานวิจัยนี้กาารคำนวณโดยใช้ฟังก์ชันนัลแบบผสมถูกใช้ในการตรวจสอบเสถียรภาพและผลกระทบของในโ ตรเจนที่เจือปนในผลึก SrTiO<sub>3</sub> ที่มีต่อคุณสมบัติเชิงอิเล็กทรอนิกส์และเชิงแสง ผู้วิจัยพบว่าในโตรเจนที่ไปแทนที่ออกซิเจน (N<sub>o</sub>) เป็นตัวรับอิเล็กตรอนแบบลึก โดยที่ N<sub>o</sub>

มีความเข้มขันสูงกว่าความบกพร่องในโตรเจนในรูปแบบอื่น ๆในเงื่อนไขการปลูกผลึกภายใต้สมดุลเชิงความร้อ นใน SrTiO<sub>3</sub> ที่เป็นชนิดเอ็น ผลการวิจัยแสดงว่า N<sub>o</sub>

ทำให้เกิดการดูดกลื่นแสงในย่านที่ตามองเห็นซึ่งสอดคล้องกับผลการทดลองที่รายงานออกมา นอกจากนี้ยังพบว่าไฮโดรเจนอะตอมสามารถยึดเกาะกับ N<sub>o</sub> กลายเป็นความบกพร่องแบบซับซ้อน N<sub>o</sub>-H<sub>i</sub> และทำให้เกิดการเลื่อนไปทางสีน้ำเงินของการดูดกลื่นแสง

รูปแบบของในโตรเจนอะตอมที่เจือปนอื่น ๆก็มีส่วนในการทำให้เกิดการดูดกลืนแสงในย่านที่ตามองเห็นได้เช่น กัน

ผู้วิจัยได้คำนวณความถี่การสั่นของในโตรเจนในรูปแบบต่างๆเพื่อช่วยสนับสนุนการทดลองที่เกี่ยวข้องกับการ วัดความถี่การสั่นอีกด้วย

#### 2. Executive summary

We employed density-functional calculations to investigate the effect of nitrogen (N) impurities on the optical properties of N-doped CaTiO3, SrTiO3 and BaTiO3. The screened hybridfunctional proposed by Heyd, Scuseria, and Ernzherhof (HSE) is used to obtain the accurate band gaps, electronic structure and formation energies of the N impurities. The Hatree-Fock exchange mixing parameters were adjusted to yield the experimental band gaps for each material. The lattice constants and heat of formations are in good agreement with the experimental values. The band alignments of the three perovskites are also provided. In this project, we pay special attention to the energetics and optical properties of N impurities in SrTiO3, which is a promising candidate for hydrogen evolution under visible-light irradiation. Here, hybrid density-functional calculations are employed to investigate the stability and impact of nitrogen impurities on the electronic and optical properties in SrTiO<sub>3</sub>. We find that the substitutional N on O site (N<sub>O</sub>) is a deep acceptor in SrTiO<sub>3</sub>. N<sub>O</sub> predominates over other N-related defects under any equilibrium growth conditions in n-type SrTiO<sub>3</sub>. Our results reveal that No gives rise to visible-light absorption, in agreement with experimental observations. In addition, we find that hydrogen can bind to  $N_0$ , and that  $N_0$ -H<sub>i</sub> leads to a blueshift in the optical absorption. Other N configurations can also contribute to optical absorption in the visible range. The vibration frequencies of the different N configurations are provided to support identification by vibrational spectroscopy techniques. The optical absorption associated with  $N_{\odot}$  in BaTiO<sub>3</sub> and CaTiO<sub>3</sub> were also calculated. We find that N<sub>O</sub> in BaTiO3 gives rise to visible-light absorption while that in CaTiO<sub>3</sub> leads to absorption near ultraviolet region.

## 3. Objective

- (1) To systematically investigate the effects of N doping in SrTiO<sub>3</sub>, BaTiO<sub>3</sub>, and CaTiO<sub>3</sub> on the visible-light absorption through hybrid-density functional calculations. The special attention is paid on N impurities in SrTiO3.
- (2) To develop the effective strategies for energy band gap engineering of  $SrTiO_3$ ,  $BaTiO_3$ , and  $CaTiO_3$  for enhancing the photocatalytic  $H_2$  production from water splitting under visible-light irradiation.

#### 4. Research methodology

Our density-functional calculations were employed using Vienna abinitio simulation package (VASP). To calculate the fundamental physical properties, we adopt the primitive cell containing 5 atoms of  $SrTiO_3$ ,  $BaTiO_3$  or  $CaTiO_3$ . For the Brillouin zone integrations, a set of  $7\times7\times7$  k-point grid is used for  $SrTiO_3$ ,  $BaTiO_3$  and  $8\times8\times8$  k-point grid is used for  $CaTiO_3$ . The energy cutoff of 400 eV is used for the plane-wave expansion for  $SrTiO_3$ ,  $BaTiO_3$  and 500 eV for  $CaTiO_3$ . The Heyd-Scuseria-Ernzehof (HSE) hybrid functional was adopted in all calculations in which the Hatree-Fock (HF) mixing parameters were determined to reproduce the experimental values. For SrTiO3,  $Sr 4s^24p^65s^2$ ,  $Ti 3d^34s^1$ ,  $O 2s^22p^4$  and the N  $2s^22p^3$  were treated as valence electrons within the projector-

augmented wave (PAW) method. The use of the Hatree-Fock mixing parameter of 28% in the HSE approach yield an indirect band gap (R-) of 3.27 eV, in good agreement with the experimental value of 3.25 eV. The calculated lattice parameter of 3.913 Å, is very close to the experimental value of 3.905 Å for cubic  $SrTiO_3$ . The HSE functional has been widely adopted in studies of defects and impurities in wide-band-gap semiconductors, with overall excellent agreement between theory and experiment. The simulations of the N impurity employed a 90-atom supercell, which is a  $3\times3\times2$  repetition of the five-atom primitive cell of cubic  $SrTiO_3$ , and  $2\times2\times2$  mesh of special k-point. The energy cutoff for the planewave basis set expansion was set to 400 eV.

The likelihood of forming substitutional, interstitial or other configurations of the N impurity is determined by the formation energy as a function of oxygen ( $\mu_{\rm O}$ ) and nitrogen ( $\mu_{\rm N}$ ) chemical potentials, for all possible charge states. We calculated the thermodynamic transition level and optical transitions following the standard procedure described in Ref. For example, the formation energy of N<sub>O</sub> in charge state q is given by:

$$E^{f}(N_{O}^{q}) = E_{tot}(N_{O}^{q}) - E_{tot}(SrTiO_{3}) - \mu_{N} + \mu_{O} + qE_{F} + \Delta^{q}$$
(1.1)

where  $E_{\rm tot}({\rm N_O^q})$  is the total energy of the supercell containing one N substituted for an O site (N<sub>O</sub>).  $E_{tot}(SrTiO_3)$  is the total energy of the perfect crystal using the same supercell. The O atom that is removed from the supercell is placed in a reservoir with energy  $\mu_0$ , referenced to the total energy per atom of an isolated  $O_2$  molecule ( $\mu_O = \tilde{\mu}_O + \frac{1}{2} E_{tot} [O_2]$ ), and the N atom is taken from a reservoir with energy  $\mu_{\mathrm{N}}$  , referenced to the total energy per atom of an isolated N $_{\mathrm{2}}$  molecule  $(\mu_{\rm N} = \tilde{\mu}_{\rm N} + \frac{1}{2}E_{\rm tot}[{\rm N}_2])$ . The chemical potentials  $\tilde{\mu}_{\rm X}$  (X = Sr, Ti, O, N, H) are treated as variables and can be appropriately chosen to represent experimental conditions during growth or annealing. The Fermi level  $E_{\varepsilon}$  is the electron chemical potential, referenced to the valence band maximum (VBM). We applied the charge-state dependent correction ( $\Delta^q$ ) due to the finite size of the supercell following the approach in Ref. [37]. Notably, however,  $\Delta^q$  is very small, due to the large static dielectric constant of SrTiO<sub>3</sub>. The formation energy of the other N configurations and N-H complexes in various charge states are obtained using similar procedure. The chemical potentials  $ilde{\mu}_{ ext{Sr}}$  ,  $ilde{\mu}_{ ext{Ti}}$  and  $\tilde{\mu}_{\rm O}$  must satisfy the stability condition of  $\tilde{\mu}_{\rm Sr}$  +  $\tilde{\mu}_{\rm Ti}$  +  $3\tilde{\mu}_{\rm O}$  =  $\Delta H_f({\rm SrTiO_3})$ , where  $\Delta H_f({\rm SrTiO_3})$  is the enthalpy of formation of SrTiO<sub>3</sub>; the calculated value is -16.2 eV. Their values are taken with respect to the total energy per atom of metallic Sr (fcc), metallic Ti (hcp) and O2 molecule. Bounds are imposed to  $ilde{\mu}_{\rm Sr}$  ,  $ilde{\mu}_{\rm Ti}$  and  $ilde{\mu}_{\rm O}$  in order to avoid formation of secondary phases. For example, the formation of SrO is prevented by taking into account the constraint:  $\tilde{\mu}_{\rm Sr} + \tilde{\mu}_{\rm O} < \Delta H_f({\rm SrO})$ . Similar constraints are applied to the formation of other relevant limiting phases: SrO<sub>2</sub>, TiO<sub>2</sub>, TiO and Ti<sub>2</sub>O<sub>3</sub>.<sup>29</sup> We present results of formation energies for O-rich, the intermediate, and O-poor conditions. The Orich and O-poor conditions correspond to the oxygen chemical potential  $ilde{\mu}_0$  = 0 and  $\tilde{\mu}_{\rm O} = (\Delta H_f({\rm SrTiO_3}) - \tilde{\mu}_{\rm Ti} - \tilde{\mu}_{\rm Sr})/3 = -5.27$  eV, respectively. For the intermediate condition, the O chemical potential was chosen to reflect the growth conditions in Ref. [16]. Based on a growth

temperature of 1100  $^{\circ}$ C and a pressure of 1 atm, we get  $\tilde{\mu}_{\rm O} = -1.57$  eV. Under O-rich and the intermediate (experimental) growth conditions,  $\tilde{\mu}_{\rm N}$  is limited by the formation of N<sub>2</sub> molecule, i.e.,  $\tilde{\mu}_{\rm N} = 0$  while under O-poor (Ti-rich) growth condition,  $\tilde{\mu}_{\rm N}$  is limited by the formation of solid TiN, i.e.,  $\tilde{\mu}_{\rm N} = \Delta H_f({\rm TiN}) - \tilde{\mu}_{\rm Ti}$ . Note that the formation of NO, N<sub>2</sub>O, NO<sub>2</sub> molecules are not relevant in determining  $\tilde{\mu}_{\rm N}$  under any growth condition considered. Under O-rich and the experimental conditions, the solubility of H-related defects are limited by the formation of H<sub>2</sub>O, i.e.,  $\tilde{\mu}_{\rm H} = (\Delta H_f({\rm H_2O}) - \tilde{\mu}_{\rm O})/2$ , while under O-poor conditions (metal-rich) the solubility is limited by the formation of solid SrH<sub>2</sub>, i.e.,  $\tilde{\mu}_{\rm H} = (\Delta H_f({\rm SrH_2}) - \tilde{\mu}_{\rm Sr})/2$ . The allowed chemical potential values for BaTiO<sub>3</sub> and CaTiO<sub>3</sub> were obtained following the similar procedure. The chemical potential diagram for the stable growth of SrTiO3 is shown in Fig. 1.

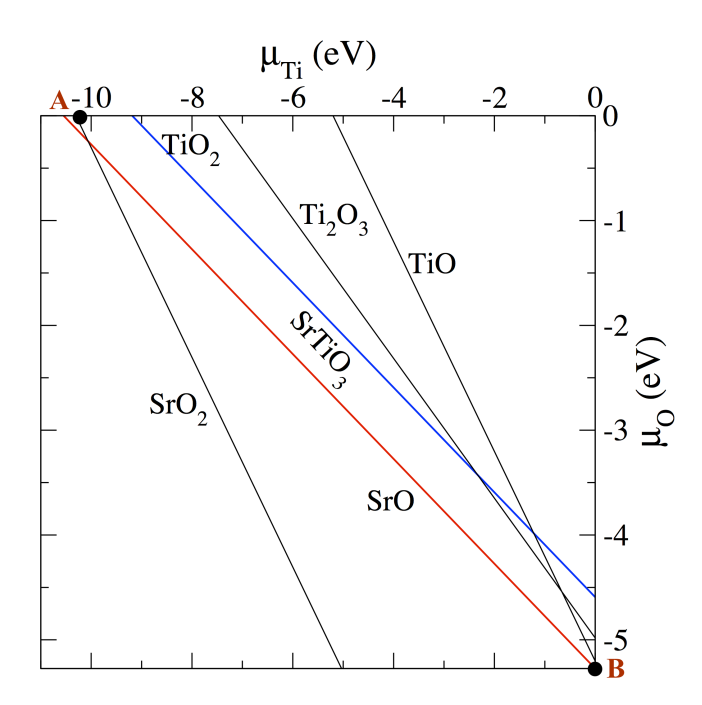


Figure 1 Chemical potentials conditions for stable growth of SrTiO<sub>3</sub> under thermodynamic equilibrium

#### 5. Results

First of all, we report the calculated fundamental properties of the three perovskites. The calculated basic physical properties, i.e., (1) lattice constant (2) heat of formation and (3) band gap are shown in Table 1-3.

Table 1 Caculated lattice parameters of  $SrTiO_3$ , energy band gap ( $E_g$ ) and formation enthalpy ( $\Delta H_s$ ) using functional PBE and HSE06, compared with the experimental values

	PBE	HSE06 $(\alpha = 0.28)$	Experiments
a (Å)	3.953	3.913	3.905
$E_g$ (eV) - indirect	1.66	3.27	3.25
- direct	2.00	3.57	3.75
$\Delta H_{_f}$ (eV)	-15.58	-16.20	-17.34

Table 2 Caculated lattice parameters of  $BaTiO_3$ , energy band gap ( $E_g$ ) and formation enthalpy ( $\Delta H_p$ ) using functional PBE and HSE06, compared with the experimental values

	PBE	HSE06 $(\alpha = 0.30)$	Experiments
a (Å) E <sub>g</sub> (eV)	4.038	3.985	4.000
- indirect	1.57	3.25	-
- direct	1.70	3.28	3.27
$\Delta H_{_f} (\mathrm{eV})$	-12.377	-15.90	-17.10

Table 3 Caculated lattice parameters of  $CaTiO_3$ , energy band gap ( $E_g$ ) and formation enthalpy ( $\Delta H_s$ ) using functional PBE and HSE06, compared with the experimental values

	PBE	HSE06 $(\alpha = 0.30)$	Experiments
a (Å)	3.897	3.851	3.840
Eg (eV)			
- indirect	1.733	3.483	3.500
- direct	2.148	3.897	-
$\Delta H_{_f}$ (eV)	-15.27	-15.90	-17.24

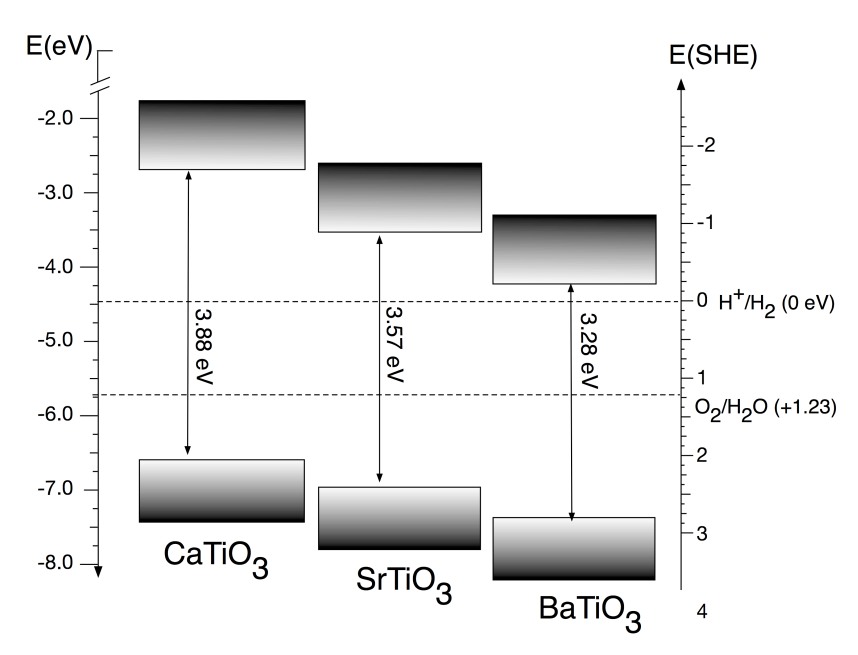


Figure 2 Calculated band offsets of CaTiO<sub>3</sub>, SrTiO<sub>3</sub> ad BaTiO<sub>3</sub>.

We find that the values of lattice constant, band gap and heat of formation obtained by HSE are in good agreement with experimental values. In particular, by properly selecting the HF parameter, the calculated band gaps of all SrTiO<sub>3</sub>, BaTiO<sub>3</sub> and CaTiO<sub>3</sub> are in excellent agreement with experimental values. We expect the HSE is capable for not only reproducing the experimental band gaps but also improving electronic structure of the materials as well as formation energy of defects and dopants.

Band offsets of CaTiO $_3$ , SrTiO $_3$  and BaTiO $_3$  are calculated using the slab models in which the non-polar TiO $_2$  terminated surfaces were adopted. In the slab models, the supercell containing 48 atom with vacuum region more than 20 Å were used. The band edge positions referenced to the vacuum level are calculated by the following procedures. (1) the energy difference between the vacuum level ( $V_{vac}$ ) and  $V_{ae}$  is calculated as  $\Delta V_{slab} = V_{vac} - V_{ae}$ , where  $V_{ae}$  is the average electrostatic potential in the bulk region of the slab. (2) the energy difference between the valence band edge position,  $E_{VB}$  and  $V_{ae}$  in the bulk unit cell is determined as  $\Delta V_{bulk} = E_{VB} - V_{ae}$ . We thus can estimate the valence band edge position as  $E_{VB}(VAC) = \Delta V_{bulk} - \Delta V_{slab}$ . The band offsets are shown in Fig.2. We find that the valence band edge position of the three perovskites are lower than the  $O_2/H_2O$  oxidation potential and the conduction band edge positions are higher than H+/H $_2$  reduction potential of water. The conduction band edge ( $E_{cbe}$ ) and valence band edge ( $E_{vbe}$ ) positions are in the order of  $E(CaTiO_3) > E(SrTiO_3) > E(BaTiO_3)$ .

Next, we address in detail the energetics and optical properties of selected N impurities in  $SrTiO_3$ , which are (1) substitutional N at O site (N<sub>O</sub>) (2) N<sub>O</sub>-H<sub>i</sub> complex, in which hydrogen binds with N<sub>O</sub> (3) (N<sub>2</sub>)<sub>2O</sub> complex and (4) (NO<sub>2</sub>)<sub>2O</sub> complex. Figure 3 shows the local atomic structures for N impurities in SrTiO3 investigated in this project. The calculated formation energies for N<sub>O</sub>, (NO)<sub>O</sub>, (NO<sub>2</sub>)<sub>2O</sub>, (N<sub>2</sub>)<sub>O</sub> and (N<sub>2</sub>)<sub>2O</sub> for the O-poor, intermediate (experimental), and O-rich conditions are shown

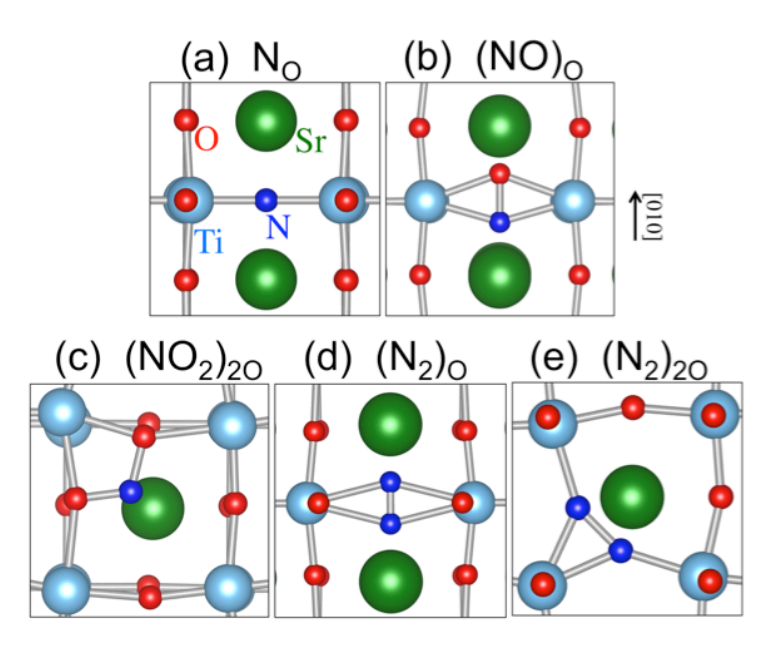


Figure 3 Local atomic structures of N impurities in  $SrTiO_3$ : (a)  $N_O$  (b)  $(NO)_O$  (c)  $(NO_2)_{2O}$  (d)  $(N_2)_O$  and (e)  $(N_2)_{2O}$ 

in Fig. 4. The formation energies for other conditions can be determined using appropriate values for the oxygen and nitrogen chemical potentials. Our calculated formation energies indicate that  $N_{\rm O}$  is the prevalent defect for Fermi-level values near the conduction band for all conditions considered.  $N_{\rm O}$  is expected to behave as an acceptor in SrTiO $_{\rm 3}$ , since N has one valence electron less than O, and can be stable in either the neutral or negative charge states. As shown in Fig. 4, we find that  $N_{\rm O}$  occurs in the neutral ( $N_{\rm O}^{\rm O}$ ) and negative charge states ( $N_{\rm O}^{\rm -}$ ), which is the most energetically favorable defect for Fermi-level values near the conduction-band minimum. This conclusion remains valid for all values of O chemical potential between O-rich and O-poor. The thermodynamic transition level (0/—) is located at 1.51 eV above the VBM, indicating that  $N_{\rm O}$  is a deep acceptor. This result is similar to the behavior of  $N_{\rm O}$  in ZnO $^{\rm 38}$  and TiO $^{\rm 28}$ , and indicates that  $N_{\rm O}$  cannot lead to p-type conductivity in SrTiO $_{\rm 3}$ .

The optical properties of  $N_{\rm O}$  center are determined through the configuration coordinate diagram as shown in Fig. 3(a). The optical transitions associated with  $N_{\rm O}$  occur through the process  $N_{\rm O}^- + hv \to N_{\rm O}^0 + e^-$  in which  $N_{\rm O}^-$  absorb a photon, converting to  $N_{\rm O}^0$  with an electron in the conduction band. The absorption energy was obtained by calculating the difference of formation energy between  $N_{\rm O}^0$  in  $N_{\rm O}^-$  lattice geometry and  $N_{\rm O}^-$  for  $E_F$  at the conduction band, and corresponds to the  $N_{\rm O}$ -related absorption peak. We find that  $N_{\rm O}$  leads to sub-band gap optical absorption peak centered at 2.46 eV, in which an electron is excited from the fully occupied states of  $N_{\rm O}^-$  (Fig. 3(b)) to the conduction band. Our calculated absorption energy of 2.46 eV is in good agreement with the experimental observations, in which the absorption edge is reported to occur at about 500 nm (~2.48 eV). The calculated emission energy, representing a recombination of an electron in the conduction band with the hole in  $N_{\rm O}^0$ , i.e.,  $N_{\rm O}^0 + e^- \to N_{\rm O}^- + hv$ , is 0.97 eV. This large difference between absorption and emission energy reflects a large Stokes shift, originating

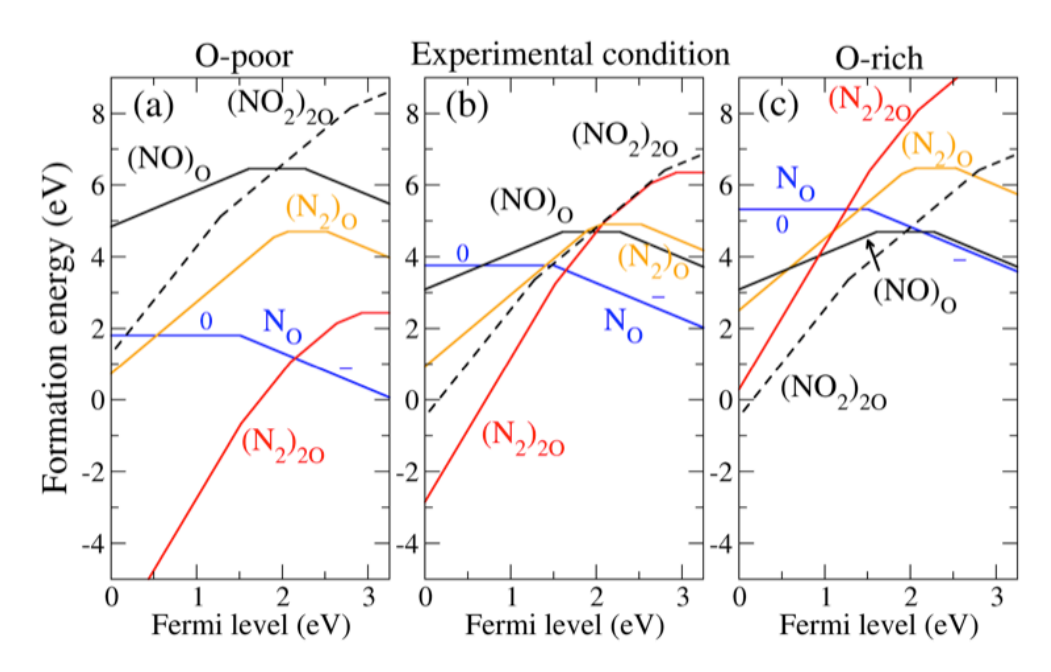


Figure 4 Formation energies of N-related defects as a function of Fermi level ranging from 0 to calculated band gap of 3.27 eV under (a) O-poor, (b) experimental and (c) O-rich growth conditions. The slopes of the line indicate the charge states of the defects.

from very different local atomic relaxations associated with  $N_O^0$  and  $N_O^-$ . We find the Ti atoms surrounding  $N_O^0$  relax outward by 1.53% with respect to equilibrium Ti-O bond length, while the Ti atoms surrounding  $N_O^-$  relax inward by 4.20 %. This large difference of local atomic relaxations also indicates that the absorption and emission peaks are quite broad. We also consider the transition through the process  $N_O^0 + hv \rightarrow N_O^- + h^+$  in which an electron is transferred to  $N_O^0$ , converting it into  $N_O^-$  with a hole in the valence band. The absorption energy can be calculated by constructing the configuration coordinate diagram in the same way, as shown in Fig. 3(a), which yields a value of 2.28 eV, slightly less than the absorption energy associated with the conduction band electron exchange. This value is in good agreement with a recent experimental observation in which the optical band gap of N-bombarded SrTiO $_3$  was reported to be 2.31 eV. In these experiments, it is likely that the Fermi level is pinned near the (0/-) transition level of  $N_O^-$ , leading to non-negligible concentrations of  $N_O^0^-$ . Both processes lead to the visible-light absorption, albeit, the process centered on  $N_O^-$  yields slightly higher absorption energy than the process centered on  $N_O^0^-$  does. In n-type SrTiO $_3$ , however, the process involving excitation of  $N_O^-$  is dominant and likely to contribute to photocatalysis processes, where an electron is excited to the conduction band.

Since hydrogen is an ubiquitous impurity and has been reported to play important role in the electrical properties of many oxides, it is worthwhile to consider the interactions between hydrogen and N in  $SrTiO_3$ . First, we find that interstitial H (H<sub>i</sub>) prefers to bind with host O without introducing any state in the band gap. It is exclusively stable in 1+ charge state (H<sub>i</sub><sup>+</sup>), acting as a shallow donor. Our calculated result for H<sub>i</sub> is in good agreement with the recent calculations based on the

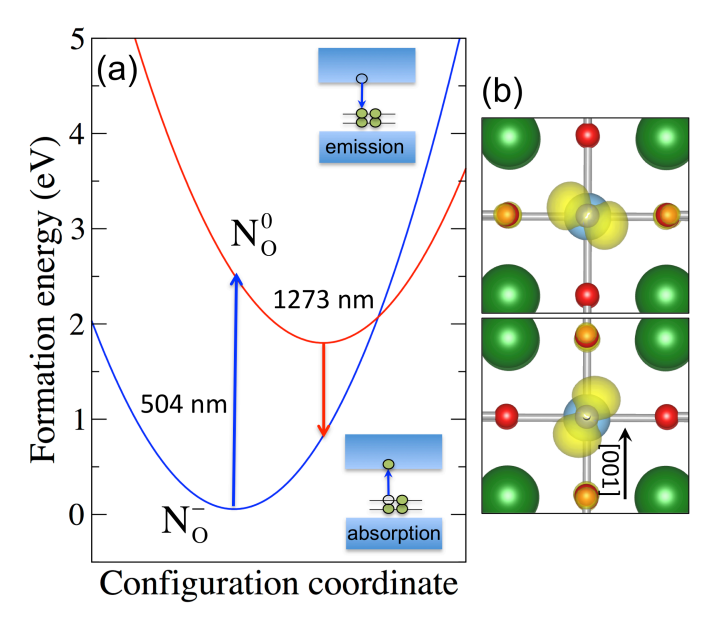


Figure 5 (a) Configuration coordinate diagram for  $N_o$ . The formation energies correspond to the similar condition in Fig. 2(a), and for  $E_F$  at the conduction-band minimum. (b) Charge distribution of  $N_o$  2p states associated with the optical transition.

 $\mathsf{HSE06}$  screened hybrid-functional. <sup>41</sup> The shallow donor behavior of  $\mathsf{H}_i$  has been also reported in other oxide semiconductors. In addition, the migration barrier for H, has been reported to be as low as 0.25 eV, indicating that it is highly mobile even at very low temperatures, unless it is trapped by other defects.  $^{42}$  We expect that  $H_i^+$  can be trapped by  $N_{\rm O}$  acceptors through Coulombic attraction. Figure 4(a) shows the calculated formation energies of N<sub>O</sub>-H<sub>i</sub> complex, H<sub>i</sub> and N<sub>O</sub> in SrTiO<sub>3</sub> under Opoor condition. We find that No-Hi occurs in 1+ and neutral charge states with the transition level (+/0) located at 1.23 eV above the VBM. This behavior of N<sub>O</sub>-H<sub>i</sub> in SrTiO<sub>3</sub> contrasts to that reported in TiO<sub>2</sub> in which N<sub>O</sub>-H<sub>i</sub> is only stable in the neutral charge state. In TiO<sub>2</sub>, H completely passivates the localized state of  $N_{\mathrm{O}}^{-}$  that appears in the band gap, whereas in  $\mathrm{SrTiO_{3}}$  H partially passivates one of the localized states of  $N_{\mathrm{O}}^{-}$ , leaving another N-related state in the band gap. Figure 5 illustrates the schematic diagram of  $N_0$  2p and  $H_i$  s hybridization in  $TiO_2$  and  $SrTiO_3$ . In  $TiO_2$ , two electrons from  $m N_{
m O}^-$  2p occupy the bonding state and lie deep in the valence band, leaving the empty antibonding state resonant in the conduction band (Fig. 5(a)). Therefore, the localized gap state is absent and  $N_0$ - $H_i$  can only be stable in the neutral charge state. In  $SrTiO_3$ ,  $N_0^-$  induces two nearly-degenerated states, fully occupied by four electrons. This is a result of the difference in coordination number between TiO2 and SrTiO3; in TiO2 N is threefold coordinated, while in SrTiO3 N is twofold coordinated. Thus, two non-bonding states are present in the band gap in the case of SrTiO3 while only one non-bonding state is present in the case of TiO2. While one of the two occupied state participates in N<sub>O</sub> 2p and H<sub>i</sub> s hybridization in SrTiO<sub>3</sub>, another state does not and resides in the band gap (Fig. 5(b)). An electron can be removed from this state, resulting in  $(N_0 - H_i)^+$ . We also consider the optical transition associated with the process  $(N_O - H_i)^0 + hv \rightarrow (N_O - H_i)^+ + e^-$ , in

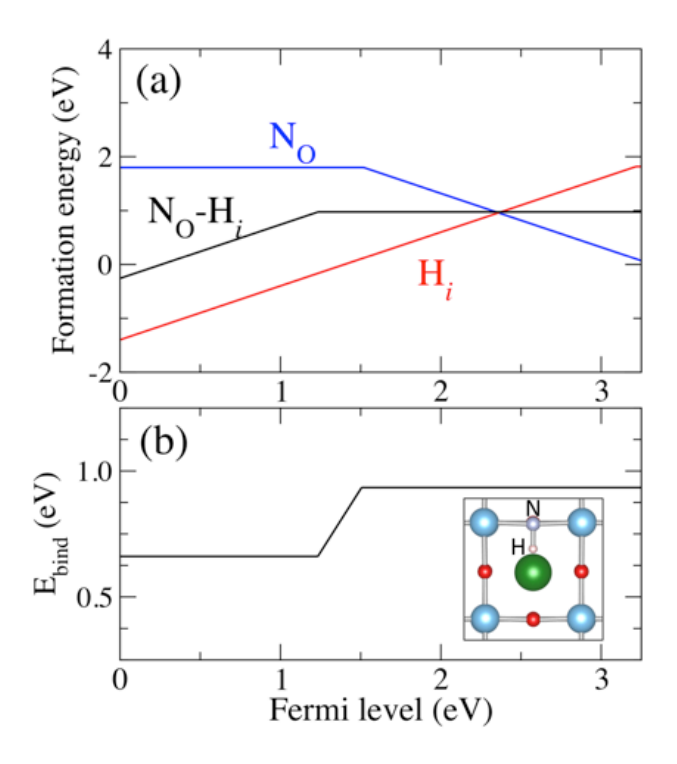


Figure 6 (a) Formation energies of  $N_O$  and  $H_i$  and  $N_O$ - $H_i$  complex under the O-poor condition and (b) calculated binding energy of  $N_O$ - $H_i$  as a function of Fermi level (see more details in the text). Inset shows the local atomic structure of  $N_O$ - $H_i$ .

which an electron is excited from  $(N_O - H_i)^0$  to the conduction band. The calculated absorption energy is 2.76 eV, higher than the absorption energy associated with  $N_O$ . This absorption energy is in good agreement with the experimental observations in N-doped  $SrTiO_3$  samples that either highly contain hydrogen<sup>16</sup> or used  $NH_3$  as nitridizing source.<sup>43</sup>

We also calculated the binding energy of the N<sub>O</sub>-H<sub>i</sub> complex, defined as:

$$E_b[(N_O - H_i)^q] = E^f[N_O^{q'}] + E^f[H_i^+] - E^f[(N_O - H_i)^q]$$
(1.2)

where  $E^f[(N_O-H_i)^q]$  is the formation energy of the complex in charge state q (q = 0, +).  $E^f[N_O^{q'}]$  is the formation energy of  $N_O$  in charge state q' (q' = 0, -). The calculated binding energy as a function of Fermi level is shown in Fig 4(b). The binding energy for  $(N_O-H_i)^0$  is 0.94 eV, higher than that in  $TiO_2$  (0.58 eV in rutile and 0.49 eV in anatase). However, it is only 0.66 eV for  $(N_O-H_i)^+$ , when the Fermi level moves toward the valence band. Note that the binding energies remain unchanged for higher O chemical potentials. To address the stability of the complex, we estimated its dissociation energy, given by  $E_b[(N_O-H_i)^0]+E_m(H_i^+)$ , to be 1.2 eV, where  $E_m(H_i^+)$  is the calculated migration barrier of interstitial hydrogen of 0.25 eV.  $N_O-H_i^0$  is thus expected to be stable at temperatures of up to ~465 K. Our results indicate that the presence of H does not

completely reverses the visible light-absorption capability of N-doped SrTiO<sub>3</sub>, instead it results in blueshifted absorption edge.

We also investigated the interaction between the two nearby substitutional N on O sites  $(N_0-N_0)$ . We find that, through large lattice relaxations, the two No are coupled and spontaneously combine into a configuration of  $N_2$  split-interstitial. This complex is denoted as  $(N_2)_{20}$  and shown in Fig. 1(e). Recently, the coupling of two  $N_0$  in  $TiO_2^{40}$  and  $SrTiO_3^{26}$  were studied, however, the energetics of (N<sub>2</sub>)<sub>20</sub> in charge states other than neutral and under different growth conditions were not considered, and the optical absorption was determined based on calculating absorption coefficient using dielectric tensors.  $(N_2)_{20}$  in neutral charge state introduces two fully occupied states in the band gap. These electrons can be removed when the Fermi level moves toward the valence band. We thus find that  $(N_2)_{20}$  can be stable in 4+, 3+, 2+, 1+ and neutral charge states with the transition levels (4+/3+), (3+/2+), (2+/+) and (+/0) at 1.52 eV, 2.09 eV, 2.64 eV and 2.93 eV above the VBM, respectively. Since substituting two O atoms are involved in the creation of  $(N_2)_{20}$ , under the O-poor conditions  $(N_2)_{20}$  has lower formation energy than  $(N_2)_0$  for all Fermi-level positions in the band gap. In addition, we examine the relative stability of  $(N_2)_{20}$  complex with respect to two isolated  $N_0$  by calculating the binding energy defined as  $E_b = 2E^f[N_0^0] - E^f[(N_2)_{20}^0]$ . A positive value of binding energy means that the neutral  $(N_2)_0$  is lower in energy than the isolated neutral  $N_0$ . Our calculated binding energy for  $(N_2)_0$  in  $SrTiO_3$  is 1.17 eV, slightly smaller than the value reported in Ref. <sup>26</sup>. To examine the optical transitions associated with (N2)20, we considered processes involving electron transfer from the valence band to the defect state and from the defect state to the conduction band, i.e., (1)  $(N_2)_{20}^{3+} + hv \rightarrow (N_2)_{20}^{2+} + h^+$ , in which an electron is excited from the valence band into  $(N_2)_{20}^{3+}$ , leaving a hole in the valence band; (2)  $(N_2)_{20}^{3+} + hv \rightarrow (N_2)_{20}^{4+} + e^-$ , in which an electron is excited from  $(N_2)_{20}^{3+}$  to the conduction band; (3)  $(N_2)_{20}^{4+} + hv \rightarrow (N_2)_{20}^{3+} + h^+$ , in which an electron is excited from the valence band into  $(N_2)_{20}^{4+}$ , leaving a hole. These processes yield the absorption energies of 2.77 eV, 2.61 eV and 2.52 eV, respectively, which fall into the visible-light region. Figure 2 shows that  $(N_2)_{20}$  and  $N_0$  are dominant defects under O-poor and experimental conditions. At Fermi level about 2.15 and 1.63 eV above the VBM, which correspond to the intersections of the two formation energy lines for  $N_0$  and  $(N_2)_{20}$ , the concentrations of  $(N_2)_{20}$  and  $N_0$  are the same. This means that  $N_0$  and  $(N_2)_{20}$  can comparably contribute to the light absorption in visible range in  $SrTiO_3$ samples with Fermi-level positions near these values. Note that the formation energy of  $(N_2)_{20}$  will decrease as twice as that of No when N chemical potential is raised. Therefore, in case of high-N doping,  $(N_2)_{20}$  could become the dominant defect in a wider range of Fermi level (see Fig. S1). <sup>39</sup> We thus cannot exclude that  $(N_2)_{20}$  can serve as a source of visible-light absorption in N-doped SrTiO<sub>3</sub>. In addition, Figure 2 shows that  $(N_2)_{20}$  which is a quadruple donor can be compensating center for No acceptor under O-poor and experimental conditions. This is because, the Fermi level will be pinned at about the intersections of the two formation energy lines for predominant N-related defects: N<sub>O</sub> (acceptor) and (N<sub>2</sub>)<sub>2O</sub> (donor), at which a charge neutrality of the system is nearly satisfied among negatively charged  $N_0$  and positively ionized  $(N_2)_{20}$ . Note that the free electron and

hole carriers were neglected in determining the pinned Fermi level because of the wide band gap of  $SrTiO_3$ . These pinned Fermi levels, which locate in the middle of the band gap far away from the VBM, indicate that hole carrier concentration is extremely low. Combined our results for  $N_0$ , which is a deep acceptor, and  $(N_2)_{20}$ , which acts as active compensating center, we thus believe that N-doped  $SrTiO_3$  cannot become p-type under these conditions.

In addition to split interstitial configuration, we find that N can bind with two nearby host O atoms, forming NO<sub>2</sub>-like configuration (NO<sub>2</sub>)<sub>20</sub> (Fig. 1(c)), which is energetically stable in 1+, 2+ and 3+ charge states. Under O-rich condition, (NO<sub>2</sub>)<sub>20</sub> has relatively low formation energy for Fermi-level positions in the lower half of the band gap (Fig. 2(c)), indicating that it could exist with a significant concentration in SrTiO<sub>3</sub> that is grown under high oxygen partial pressures and Fermi level positions below ~1.9 eV with respect to the VBM. Optical transitions of (NO<sub>2</sub>)<sub>20</sub> are considered to occur via the process  $(NO_2)_{20}^{2+} + hv \rightarrow (NO_2)_{20}^{3+} + e^-$ , in which an electron is excited from  $(NO_2)_{20}^{2+}$  to the conduction band and the process  $(NO_2)_{20}^{3+} + hv \rightarrow (NO_2)_{20}^{2+} + h^+$ , in which an electron is excited from the valence band to  $(NO_2)_{20}^{3+}$ . These processes give absorption energies of 2.80 eV and 2.19 eV, respectively. It is thus possible that  $(NO_2)_{20}$  contributes to the optical absorption in the visible region in some SrTiO<sub>3</sub> samples.

Finally, the optical transitions associated with  $N_{\rm O}$  in CaTiO3 and BaTiO3 were also examined. We find that  $N_{\rm O}$  leads to sub-band gap optical transitions at 3.10 for CaTiO3, 2.23 for SrTiO3, and 2.15 eV for BaTiO3. The near ultraviolet absorption of  $N_{\rm O}$  in CaTiO3 indicates that the  $N_{\rm O}$  levels are reasonably close to the valence band maximum compared to those in SrTiO3 and BaTiO3 where the photon absorption is in the visible-light region.

#### 6. Conclusion and Discussion

In summary, based on hybrid-density functional calculations, we have investigated the thermodynamic stability and the effects of N impurities on optical absorption in  $SrTiO_3$ . We find that substitutional  $N_0$  is a deep acceptor and energetically favorable over other N impurity configurations in n-type  $SrTiO_3$ . Our calculations show that  $N_0$  gives rise to optical absorption in the visible region, consistent with the experimental observations. We also find that hydrogen can bind with  $N_0$ . In contrast to  $TiO_2$ , formation of  $N_0$ - $H_i$  complex does not completely reverses the  $N_0$ -induced visible-light absorption, yet it leads to a blueshift in the absorption edge. Our results indicate that  $N_0$ - $H_i$  can explain the observed optical absorption in the samples prepared with highly-H contained nitridizing sources. Higher binding energy of  $N_0$ - $H_i$  in  $SrTiO_3$  compared to that in  $TiO_2$  indicates that thermal annealing at higher temperatures is needed to remove H, restoring the optical properties of  $N_0$ . Our results suggest that the other possible N configurations also contribute to optical absorption in the visible range. In addition, we find that  $(N_2)_{20}$  acts as active compensating donor for  $N_0$  acceptor; thus it is very unlikely to use N for p-type doping. In addition, we investigate optical absorption associated with  $N_0$  in  $CaTiO_3$  and  $BaTiO_3$ . The near ultraviolet absorption is found in  $CaTiO_3$  whereas visible-light absorption is found in  $BaTiO_3$  quite similar with  $SrTiO_3$  case.

## 7. Output (Acknowledge the Thailand Research Fund)

- 7.1 International Journal Publication
- (1) Pakpoom Reunchan, Naoto Umezawa, Anderson Janotti, Jiraroj T-Thienprasert, Sukit Limpijumnong. Energetics and optical properties of nitrogen impurities in SrTiO<sub>3</sub> from hybrid density-functional calculations. Physical Review B **95**, 205204 (2017) [included in Appendix].
  - 7.2 International conference
- (1) Pakpoom Reunchan, Naoto Umezawa, Anderson Janotti, Jiraroj T-Thienprasert, Sukit Limpijumnong. Energetics and optical properties of nitrogen impurities in SrTiO<sub>3</sub> from hybrid density-functional calculations. 29<sup>th</sup> International Conference on Defects in Semiconductors, July 31 August 4, 2017, Matsue, Shimane prefecture, Japan. [Poster presentation].